Regenerative Therapy 5 (2016) 64–71

Contents lists available at ScienceDirect

Regenerative Therapy

journal homepage: http://www.elsevier.com/locate/reth

Original Article

Preparation of a nitric oxide imaging agent from gelatin derivative micelles

Mikio Tatsutomi, Jun-ichiro Jo, Yasuhiko Tabata*

Department of Biomaterials, Institute for Frontier Medical Sciences, Kyoto University, 53 Kawara-cho Shogoin, Sakyo-ku, Kyoto 606-8507, Japan

ARTICLE INFO

Article history:
Received 7 June 2016
Received in revised form
14 July 2016
Accepted 15 August 2016

Keywords:
Gelatin
Polymer micelles
Water-solubilization
Fluorescent dye
Nitric oxide
Macrophages

ABSTRACT

Introduction: Nitric oxide (NO) is an intracellular and intercellular messenger that plays an important role in cellular events in physiological and pathophysiological processes. NO is one of the inflammation markers and macrophages of an inflammatory cell produce a large amount of NO compared with other cells. Non-invasive detection system of NO is highly required to realize an early therapeutic treatment considering the process of pathophysiological changes. The objective of this study is to develop an imaging agent of nitric oxide (NO).

Methods: A water-insoluble DAR-4M of fluorescent dye for NO was solubilized in water through the micelle formation with gelatin grafted with L-α-phosphatidylethanolamine distearoyl (DAR-4M micelles). Physicochemical and biological properties of DAR-4M micelles were investigated by using cultured cells and animals.

Results: The DAR-4M micelles responded to NO secreted from a NO donors, in contrast to the same concentration of free DAR-4M. When RAW264.7 of a macrophage cell line was stimulated by lipopolysaccharide (LPS) to allow them to generate NO, the DAR-4M micelles could detect NO of the cells to a significant great extent compared with free DAR-4M. After the intravenous injection of DAR-4M micelles or free DAR-4M to a mouse model of aristolochic acid (AA) induced acute interstitial nephritis, the DAR-4M micelles enhanced the fluorescence intensity from the kidneys to a significant great extent compared with the free DAR-4M injection. In case of DAR-4M micelles injection into normal mice, such an enhanced kidney fluorescence was not observed. A body distribution experiment demonstrated that the kidney accumulation of DAR-4M micelles was not modified by the AA-induced inflammation. After the AA injection, the number of CD11b-positive cells increased with time, indicating the increased number of inflammatory macrophages.

Conclusion: DAR-4M micelles are effective in imaging NO generated from macrophages accompanied with inflammation.

1. Introduction

Inflammation is one of the biological responses to various exogenous and endogenous stimuli which cause the cellular and tissue injuries. Recently, it has been demonstrated that the inflammation and regeneration are strongly related to each other [1]. For example, the regeneration is not occurred without inflammation. The extent and duration of inflammation reaction affect the subsequent regeneration process. In this context, it is no doubt that the inflammation imaging contributes to the development of efficient regenerative therapy. Macrophages are one of immune cells which play a critical role in inflammation responses by modulating the biological functions [2]. Therefore, it is important to develop the materials and technologies to control and visualize the biological functions of macrophages.

Nitric oxide (NO) is an intracellular and intercellular messenger that plays an important role in cellular events in physiological and pathophysiological processes [3–6]. NO acts as a vascular relaxing agent, a neurotransmitter, and an inhibitor of platelet aggregation. In addition, it is recognized that NO is generated during immune and inflammatory responses [7]. It functions in innate immunity as

* Corresponding author. Department of Biomaterials, Field of Tissue Engineering, Institute for Frontier Medical Sciences, Kyoto University, 53 Kawara-cho Shogoin, Sakyo-ku, Kyoto 606-8507, Japan. Fax: +81 75 751 4646.
E-mail address: yasuhiko@frontier.kyoto-u.ac.jp (Y. Tabata).

Peer review under responsibility of the Japanese Society for Regenerative Medicine.

http://dx.doi.org/10.1016/j.reth.2016.08.003

Abbreviations

NO	nitric oxide
nNOS	neuronal NOS
eNOS	endothelial NOS
DSPE	L-α-phosphatidylethanolamine distearoyl
DSPE-NHS	N-(Succinimidyloxy-glutaryl)-DSPE
LPS	lipopolysaccharide
SNP	nitroprusside
EtOH	ethanol
aDMSO	anhydrous dimethyl sulfoxide
DDW	double-distilled water
DMEM	Dulbecco's Modified Eagle Medium
FCS	fetal calf serum
WST-8	2-(2-methoxy-4-nitrophenyl)-3-(4-nitrophenyl)-5-(2,4-disulfophenyl) -2H- etrazolium
AA	aristolochic acid
HBSS	Hank's balanced salt solution
7-AAD	7-Amino-Actinomycin D
CMC	critical micellar concentration

a toxic agent towards infectious organisms, while it can induce or regulate death and function of host immune cells. Nitric oxide synthase (NOS) of enzyme to generate NO has been extensively investigated [8–10]. NO is generally biosynthesized by three isoforms of mammalian NOS [11]. Neuronal NOS (nNOS or NOS I) and endothelial NOS (eNOS or NOS III) are constitutively expressed in neuronal and endothelial cells, respectively. Both are also referred to as cNOS. Inducible NOS (iNOS or NOS II) is expressed in cells involved in inflammation, such as macrophages and microglias when stimulated by cytokines and/or endotoxins. Generally, the level of NO produced by cNOS in stimulated endothelial and neuronal cells is much lower (nanomolar [nM] range) than that generated by iNOS in macrophages (micromolar [μM] range). It is recognized that an excessive production of NO is believed to be responsible for various pathophysiologies, but very low levels of NO are needed to maintain normal physiological conditions. The NO production is closely associated with the expression of NOS [12].

Among several NO detecting dyes developed [13–17], DAR-4M is one of fluorescence dyes and has been used as the NO detecting agents in both in vitro and in vivo systems. Since the DAR-4M emits the fluorescence only in the presence of NO, the NO detection with a high signal-to-noise ratio is realized [13]. However, there are issues to be improved for the in vivo use. The DAR-4M is a small and water-insoluble molecule which is easily diffused and disappear in the body. Thus, it is practically difficult to maintain high concentrations at the site of NO to be detected. Several researches have been reported to improve the imaging efficiency of dyes by making use of materials sciences [18–21].

Gelatin is a biodegradable material and has been extensively used for food, pharmaceutical, and medical purposes. The biosafety has been proven through their long practical applications. Gelatin is a denatured form of collagen which is the most abundant component of extracellular matrix in the body tissue. The material itself and the product degraded are both biocompatible. It is also reported that the gelatin pre-coating of microspheres augments the phagocytosis of macrophages [22]. Hydrophobic derivatives of gelatins are effective in water-solubilization of water-insoluble and low-molecular weights drugs and enhancing their biological activity [23].

This study is undertaken to design the water-soluble micelles of DAR-4M for improved NO detection. The DAR-4M was solubilized in water by the micelle formation with a derivative of gelatin grafted with L-α-phosphatidylethanolamine distearoyl (DSPE) (DAR-4M micelles). The ability of DAR-4M micelles to image NO was evaluated by the in vitro cell culture with macrophages and an inflammation model at mice in vivo. We compare the NO imaging ability with that of free DAR-4M.

2. Materials and methods

2.1. Materials

Gelatin with an isoelectric point (pI) of 5.0 (weight-average molecular weight (Mw) = 10,000), prepared via an alkaline process of bovine bone (pI5 gelatin) was kindly supplied from Nitta Gelatin Co., Osaka, Japan. N-(Succinimidyloxy-glutaryl)-L-α-phosphatidylethanolamine, distearoyl (DSPE-NHS) was purchased from NOF Co., Tokyo, Japan. Diaminorhodamine-4M (DAR-4M) was purchased from Sekisui Medical Co., Ltd., Tokyo, Japan. Collagenase D was purchased from Roche diagnosis Inc., and used in the in vivo study because of its lower cytotoxicity compared with collagenase L. Lipopolysaccharide (LPS), nitroprusside (SNP) as a NO donor, and other chemicals were purchased from Wako Pure Chemical industries, Ltd., Osaka, Japan.

2.2. Synthesis of gelatin grafted with DSPE

PI5 gelatin with Mw of 10,000 (1.0 g) was dissolved in anhydrous dimethyl sulfoxide (aDMSO) at room temperature. DSPE-NHS (1.0 g) was dissolved in aDMSO at room temperature. Next, the gelatin solution in aDMSO was slowly added to the DSPE-NHS solution in aDMSO to give the DSPE/gelatin molar ratios of 1, 3, 5, and 10, and then stirred overnight at room temperature to allow DSPE to graft to gelatin. The resulting solution was dialyzed by double-distilled water (DDW) similarly for 72 h at room temperature, and freeze-dried to obtain DSPE-grafted gelatin samples (DSPE-g-gelatin). The extent of DSPE grafted to gelatin and the critical micellar concentration (CMC) of DSPE-g-gelatin were determined by the conventional molybdenum blue method to measure the phosphorus amount [24] and the fluorescence quenching of pyrene in DSPE-g-gelatin [25], respectively.

2.3. Water-solubilization of DAR-4M by DSPE-g-gelatin

DAR-4M solution (2.1 mg/ml) in aDMSO (4.0 μl) was added to 5 ml of DSPE-g-gelatin aDMSO solution (4.0 mg/ml), followed by 1 h stirring at room temperature. Then, the mixed solution was dialyzed with Spectra/Por®Dialysis Membrane MWCO: 3500 (Spectrum Laboratories, Inc, CA) against DDW for 72 h at room temperature. The dialysate obtained was centrifuged (8000 rpm, 10 min, 25 °C) to exclude the water-insoluble fraction, and freeze-dried to obtain the DAR-4M water-solubilized by DSPE-g-gelatin micelles (DAR-4M–micelles). The size of DAR-4M micelles was measured by a Zetasizer Nano ZS90 (Malvern Instruments Ltd., Malvern, UK). The amount of DAR-4M water-solubilized in each micelle was determined by measuring the absorbance of DAR-4M at the wavelength of 315 nm after dissolving each micelle in aDMSO.

2.4. Evaluation of the DAR-4M micelles response to NO donors

The response of DAR-4M micelles to NO donors was evaluated according to the conventional fluorescence measurement [13]. Briefly, DAR-4M micelles at the DAR-4M concentration of 10 μM (3.14 mg/ml) were added into 10 mM phosphate-buffered saline (PBS, pH 7.4) or SNP/PBS solution in each well of 96-well multi-well black plate (Corning Inc., Corning, NY). The fluorescent intensity of

each well was measured 1 h later using a fluorescence microplate reader (Gemini EM Fluorescence Microplate Reader, Molecular Devices, LLC). These samples were used for every experiment independently unless otherwise mentioned.

2.5. Cytotoxicity test

RAW 264.7 cells of a macrophage cell line were seeded on each well of 24 well multi-dish culture plate (Corning Inc., Corning, NY) at a density of 1×10^4 cells/cm^2 and cultured in 500 μl of Dulbecco's Modified Eagle Medium (DMEM) (Invitrogen Corporation, Ltd., Carlsbad, CA) with 10 vol% fetal calf serum (FCS) for 24 h. Next, the medium was exchanged to DMEM, and then the DAR-4M micelles and free DAR-4M in DMEM were added to each well. After 3 h incubation, the number of cells proliferated was evaluated with a 2-(2-methoxy-4-nitrophenyl)-3-(4-nitrophenyl)-5-(2,4-disulfophenyl) -2H-tetrazolium (WST-8) assay kit (Nacalai Tesque. Inc., Kyoto, Japan).

2.6. Evaluation of DAR-4M micelles response to RAW 264.7 cells

RAW264.7 cells were seeded on glass bottom dish (Matsunami Glass Ind.,Ltd., Osaka, Japan) at a density of 1×10^5 cells/cm^2 and cultured in 1 ml of DMEM medium with 10 vol% FCS for 24 h. The medium was exchanged to DMEM containing 100 ng/ml of LPS, and incubated further for 24 h. Next, the medium was exchanged to FCS-free DMEM, and then, free DAR-4M, DSPE-g-gelatin, the mixture of free DAR-4M and DSPE-g-gelatin, or DAR-4M micelles were added to each dish. After 1 h incubation, cells were washed with PBS. The cells were viewed on a Nikon ECLIPSE 90i confocal laser scanning microscope (Nikon Corp., Tokyo, Japan).

To evaluate the fluorescent intensity of cells incubated for 1 h with free DAR-4M, DSPE-g-gelatin, the mixture of free DAR-4M and DSPE-g-gelatin, and DAR-4M micelles, RAW264.7 cells were seeded on each well of 24 well multi-dish culture plate (Corning Inc., Corning, NY) at a density of 1×10^5 cells/cm^2 cultured in 1 ml of DMEM with 10 vol% FCS for 24 h. Then, the medium was exchanged to FCS-free DMEM, and free DAR-4M, DSPE-g-gelatin, the mixture of free DAR-4M and DSPE-g-gelatin or DAR-4M micelles were added to each well. After 1 h incubation, cells were washed with PBS. The cells were viewed on a Nikon ECLIPSE 90i confocal laser scanning microscope (Nikon Corp., Tokyo, Japan).

2.7. Observation of DAR-4M micelles localization in RAW 264.7 cells

The intracellular localization of DAR-4M micelles was detected using LysoTracker Green DND-26 (Life Technologies Japan.,Ltd., Tokyo, Japan) according to the product manual. Briefly, RAW264.7 cells were seeded on glass bottom dish (Matsunami Glass Ind.,Ltd., Osaka, Japan) at a density of 1×10^5 cells/cm^2 and cultured in 1 ml of DMEM medium with 10 vol% FCS for 24 h. The medium was exchanged to DMEM containing 100 ng/ml of LPS, and incubated further for 24 h. Next, the medium was exchanged to FCS-free DMEM containing 75 nM of LysoTracker Green DND-26, and then, DAR-4M micelles were added to each dish. After 1 h incubation, cells were washed with PBS. The cells were viewed on a Nikon ECLIPSE 90i confocal laser scanning microscope (Nikon Corp., Tokyo, Japan).

2.8. Animal experiments with a model of aristlochic acid-induced kidney inflammation model

A mouse model of aristolochic acid (AA) induced interstitial nephritis was prepared as the inflammation animal [26]. All the animal experimentation was conducted in accordance with the Guidance of the Institute for Frontier Medical Sciences, Kyoto University. After 1 week of acclimatization, mice were intraperitoneally injected with AA solution in saline (5 mg/kg body weight) (AA group) or with the saline alone (original group). Imaging assay was performed 1, 4, 7, 14, 21, and 35 days after AA treatment. In vivo fluorescence images was performed by IVIS Spectrum (PerkinElmer Inc., Waltham, MA) at the excitation and emission wavelengths of 535 and 580 nm, respectively. DAR-4M micelles (3.14 mg/ml, 10 μM of DAR-4M, 200 μl) and free DAR-4M (10 μM of DAR-4M, 200 ul) were injected into the tail vein of mice (2 nmole DAR-4M/mice) at the days indicated above. Mice were sacrificed 1 h later, and the kidneys were isolated, followed by the fluorescence imaging on IVIS Spectrum. To determine the fluorescence intensity of the AA-treated and normal kidneys, the kidneys isolated was assessed by the IVIS Spectrum.

2.9. Flow cytometry of kidney cells

To quantitatively analyze the type of inflammatory cells infiltrated into the AA kidney, kidneys were enzymatically digested to prepare the cell suspensions [27], followed by the analysis of flow cytometry (FACSCanto II flow cytometer BD Biosciences, Co., Tokyo, Japan). Briefly, kidneys were dissected, placed in Hank's Balanced Salt Solution (HBSS) containing 1.6 mg/ml collagenase D for 30 min at 37 °C, and then washed twice in HBSS. Following the erythrocyte lysis with lysis buffer (BD Pharm Lyse, BD Biosciences Ltd., Rockville, MD), cells were resuspended in PBS containing 2 vol % FBS and 0.1 vol% sodium azide (FACS buffer). The kidney cells suspension was blocked by anti-CD16/32 antibody (BioLegend Ltd., San Diego, CA), washed, and stained with an anti-CD11b antibody (BioLegend Ltd., San Diego, CA), an anti-CD 45 antibody against CD45 expressed on the surface of mouse macrophages (BioLegend Ltd., San Diego, CA) in FACS buffer. 7-Amino-Actinomycin D (7-AAD, BD Biosciences Ltd., Rockville, MD) was used to distinguish dead cells from viable cells. The immunostained cells were analyzed on FACS, and the analysis was performed by the BD FACSDiva software (v6.13 BD FACSDiva software, BD Biosciences Ltd., Rockville, MD).

2.10. Evaluation of body distribution

The body distribution of DAR-4M micelles was evaluated by use of ^{125}I-labeled DAR-4M micelles. Briefly, DAR-4M micelles were labeled with ^{125}I according to the method reported previously [28]. The ^{125}I-labeled DAR-4M micelles were intravenously injected into mice 1, 4, 7, 21, and 35 days after AA treatment. The mice were sacrificed 1 h after injection of ^{125}I-labeled DAR-4M micelles, and the tissues and organs were excised. Then, the radioactivity of tissues and organs was counted by a gamma counter (Auto Well Gamma System ARC-380 CL, Aloka Co., Ltd, Tokyo, Japan). The percentage of radioactivity was expressed as 100% for the radioactivity of antibody initially injected.

2.11. Statistical analysis

Data were expressed as the means ± standard deviations. They were analyzed using Tukey–Kramer paired comparison test, while the significance was accepted at $p < 0.05$.

3. Results

3.1. Characterization of gelatin derivatives and DAR-4M micelles

Table 1 shows the preparation conditions and characterization of DSPE-g-gelatin and DAR-4M micelles. The amount of DSPE added was in a good accordance with the percentage of DSPE introduced.

Table 1
Physicochemical properties of DSPE-g-gelatin and DAR-4M micelles.

Sample code	DSPE-g-gelatin			DAR-4M micelles	
	DSPE-NHS added (mole/mole gelatin)	Percentage of DSPE grafted (mole/mole gelatin)	Critical micellar concentration (μg/ml)	Amount of DAR-4M water-solubilized (mmole/mole gelatin)	Size (nm)
DSPE-1	1	18.5 ± 1.8[a]	11.4 ± 0.2[a]	21.8 ± 4.9[a]	30.4 ± 9.1[a]
DSPE-3	3	46.6 ± 3.6	9.4 ± 0.2	42.4 ± 5.0	80.8 ± 32
DSPE-5	5	75.2 ± 2.5	4.7 ± 0.1	48.5 ± 5.2	124 ± 44
DSPE-10	10	100 ± 4.1	3.3 ± 0.1	65.2 ± 5.3	105 ± 35

[a] Mean ± SD.

The critical micellar concentration (CMC) became lower as the amount of DSPE introduced increased. The amount of DAR-4M introduced into the DSPE-g-gelatin micelles became larger with an increase in the amount of DSPE introduced. The diameter of DAR-4M micelles ranged from 30 nm to 125 nm. The DAR-4M micelles prepared from the DSPE-10 gelatin showed the largest amount of DAR-4M incorporated, while the diameter was around 100 nm. Based on this, the DAR-4M micelles of DSPE-10 were used for the following experiments.

3.2. NO reactivity of DAR-4M micelles

Fig. 1 shows the effect of DAR-4M concentration on the reactivity of free DAR-4M or DAR-4M micelles to NO produced from NO donors. Irrespective of the DAR-4M concentration, free DAR-4M responded to the NO donor. On the other hand, DAR-4M micelles weakly responded to SNP at any concentration.

3.3. In vitro evaluation of DAR-4M micelles imaging ability

Fig. 2 shows the cytotoxicity of DAR-4M micelles. The DAR-4M micelles at concentrations less than 5 μM did not have any significant cytotoxicity.

Fig. 3 shows the confocal laser microscopic pictures of RAW 264.7 cells. For free DAR-4M, LPS-stimulated RAW264.7 cells produced NO and the production was detected (A and E). When DSPE-g-gelatin alone were added to cells with or without LPS stimulation, no fluorescence was observed for both the groups (B and F). For the mixture of DSPE-g-gelatin micelles and free DAR-4M, fluorescence was observed only for the cells with LPS stimulation (C and G). When DAR-4M micelles were added to cells with or without LPS stimulation, fluorescence was observed only for LPS-stimulated cells, but not for cells without LPS stimulation (D and H).

Fig. 4 shows the fluorescent intensity of LPS stimulated RAW264.7 cells incubated with free DAR-4M, DSPE grafted-gelatin micelle with free DAR-4M, or DAR-4M micelle. For every group, the higher fluorescent intensity was observed at higher concentrations of DAR-4M added. At the same concentration of DAR-4M, significantly stronger fluorescence was detected for the DAR-4M micelles groups.

Fig. 5 shows the confocal laser microscopic picture of RAW 264.7 cells incubated with LysoTracker Green DND-26 and DAR-4M micelles. The fluorescence of DAR-4M micelles themselves merged with that of DND-26. The DAR-4M micelles were localized in the phagolysosome of cells.

3.4. In vivo evaluation of DAR-4M micelles imaging ability

Fig. 6 shows the IVIS images of isolated kidneys of mice 1 h after intravenous injection of free DAR-4M and DAR-4M micelles. Mice were treated with AA for 1, 4, 7, 21, and 35 days. When free DAR-4M was injected into mice, there was not a big difference in the fluorescent intensity between the inflamed and normal kidneys. On the contrary, for the DAR-4M micelles injection, there was significant difference in the fluorescent intensity between the two kidneys. Moreover, the fluorescence intensity of isolated kidney increased with time after AA treatment. The fluorescence intensity was higher for the DAR-4M-micelles group than for the free DAR-4M group. Fig. 7 shows percentage of CD11b-positive cells to the total live cells in the kidneys. The percentage of CD11b-positive cells in kidney inflamed increased with time.

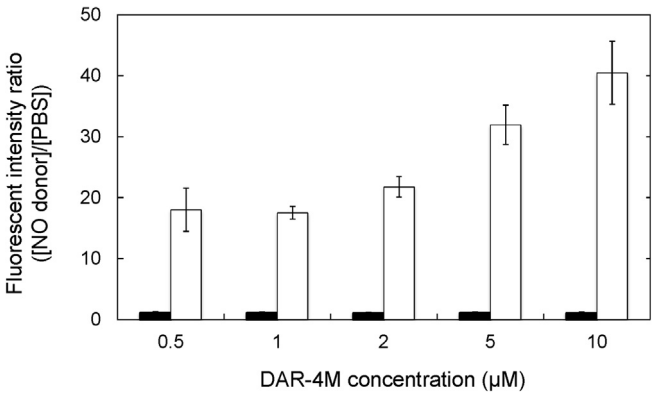

Fig. 1. Effect of DAR-4M concentration on the reactivity of DAR-4M micelles (■) or free DAR-4M (□) to NO donors. The DAR-4M micelles were prepared by DSPE-10. The fluorescent intensity ratio was calculated as the fluorescence intensity of 1.0 for the group in NO-donor-free PBS at the corresponding DAR-4M concentration. *p < 0.05; significance between the two groups.

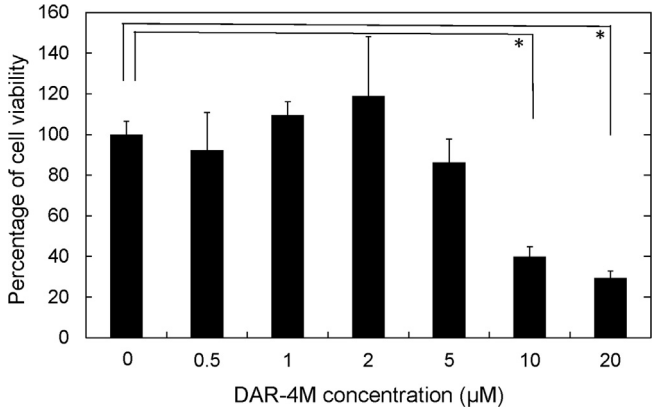

Fig. 2. Effect of the DAR-4M micelles concentration on the viability of RAW264.7 cells 3 h after incubation. The DAR-4M micelles were prepared at DAR-4M concentrations of 0.5, 1, 2, 5, 10, and 20 μM. The viability of cells cultured without DAR-4M micelles (DAR-4M concentration = 0) is indicated as 100%. *, p < 0.05; significant against the viability of cells cultured without DAR-4M micelles.

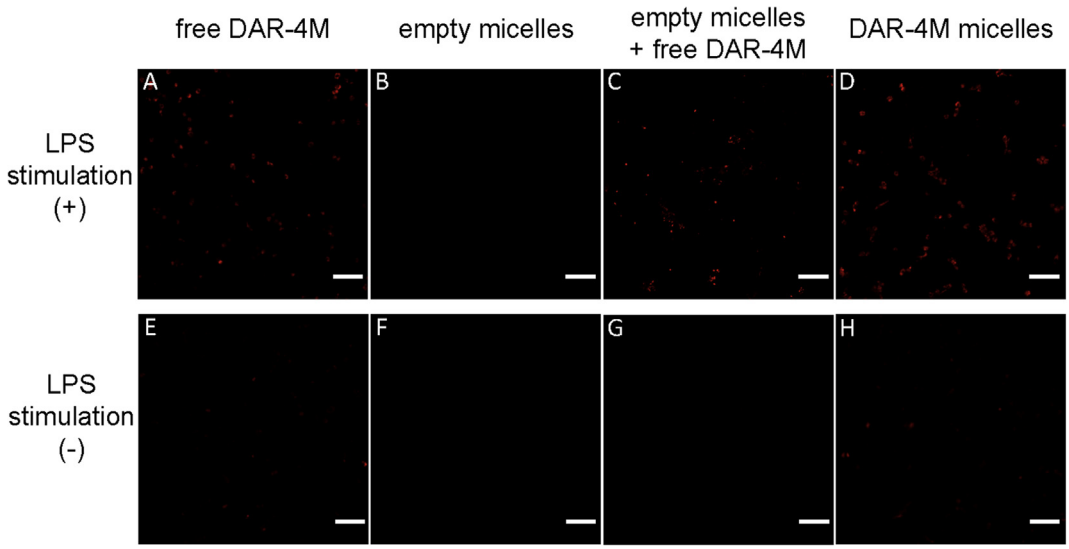

Fig. 3. Confocal laser microscopic pictures of RAW264.7 cells 1 h after incubation with (A, E) free DAR-4M, (B, F) DSPE-10, (C, G) the mixture of free DAR-4M and DSPE-10, and (D, H) DAR-4M micelles. Cells were stimulated for 24 h by 100 ng/mL of LPS (A, B, C, D) and not (E, F, G, H). The DAR-4M micelles were prepared by DSPE-10. Scale bar is 50 mm.

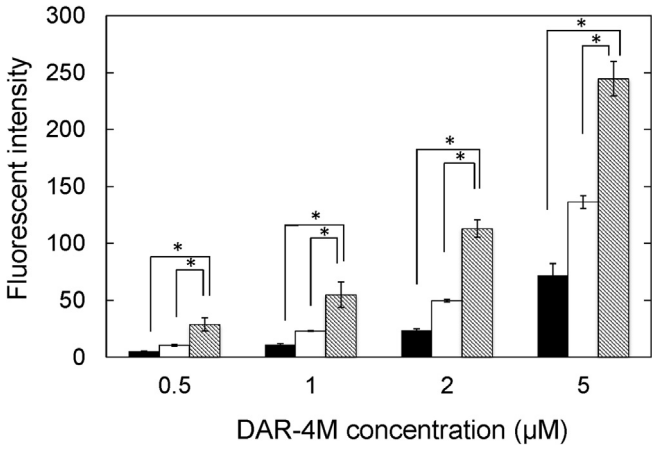

Fig. 4. Fluorescent intensity of LPS-stimulated cells 1 h after incubation with free DAR-4M (■), the mixture of free DAR-4m and DSPE-10 (□), and DAR-4M micelles (▨). The LPS concentration is 100 ng/ml. The DAR-4M micelles were prepared by DSPE-10. *$p < 0.05$; significance between the two groups.

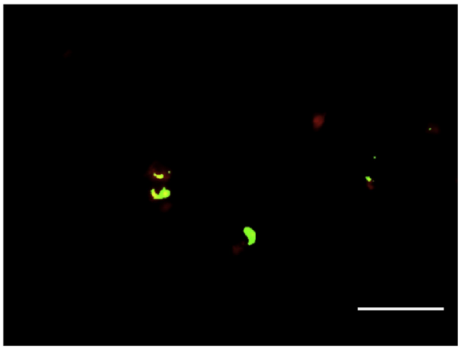

Fig. 5. Confocal laser microscopic pictures of cells 1 h after incubation with DAR-4M micelles. Red: DAR-4M. Green: lysosome. Scale bar is 50 μm.

Fig. 8 shows the body distribution pattern after the injection of ^{125}I-labeled DAR-4M micelles. Little difference in the profile of kidney accumulation was observed at different time intervals after AA treatment.

4. Discussion

The present study demonstrates that DAR-4M incorporated into the micelles of DSPE-g-gelatin micelles could detect NO effectively in both the in vitro and in vivo systems. NO could be detected at the DAR-4M concentration of 5 μM, where no significant cytotoxicity was seen (Fig. 2). The DAR-4M of a water-insoluble drug was solubilized in water by making use of the gelatin micelles. Several researches have been reported on the water-solubilization and cellular internalization of hydrophobic fluorescent dyes with different types of polymer micelles [29–32]. In this study, gelatin was selected as a starting material of polymer micelles for the following reasons. First, it has been recognized that the particles composed of or coated with gelatin are susceptible to the internalization by macrophages [22,33]. In addition, drugs encapsulated in gelatin particles can be released in the cells after their internalization [33,34].

In this study, the DSPE-10 was selected as the gelatin derivative to form DAR-4M micelles. This is because the micelles incorporated showed the highest amount of DAR-4M. In addition, the diameter of DAR-4M micelles was about 105 nm (Table 1). It is reported that the nanoparticles with sizes of 50–200 nm can be penetrated through the vascular walls of inflamed tissues and accumulated into inflamed tissue. This is called enhanced permeability and retention (EPR) effect [35,36]. Based on the points, the DAR-4M micelles of DSPE-10 gelatin derivatives was used to detect NO production in the inflammation site.

Free DAR-4M responded to NO produced by the NO donor, whereas the DAR-4M micelles hardly responded to NO (Fig. 1). This can be due to the entrapment of DAR-4M in micelles. It is conceivable that the DAR-4M is encapsulated into the micelles, resulting in no DAR-4M contact with NO to detect.

It is reported that LPS stimulation enhances the NO secretion from RAW264.7 cells [37,38]. Fluorescence was observed at the cytosol of cells even after their PBS washing. This is because DAR-4M itself is penetrated into the cytosol through the cellular

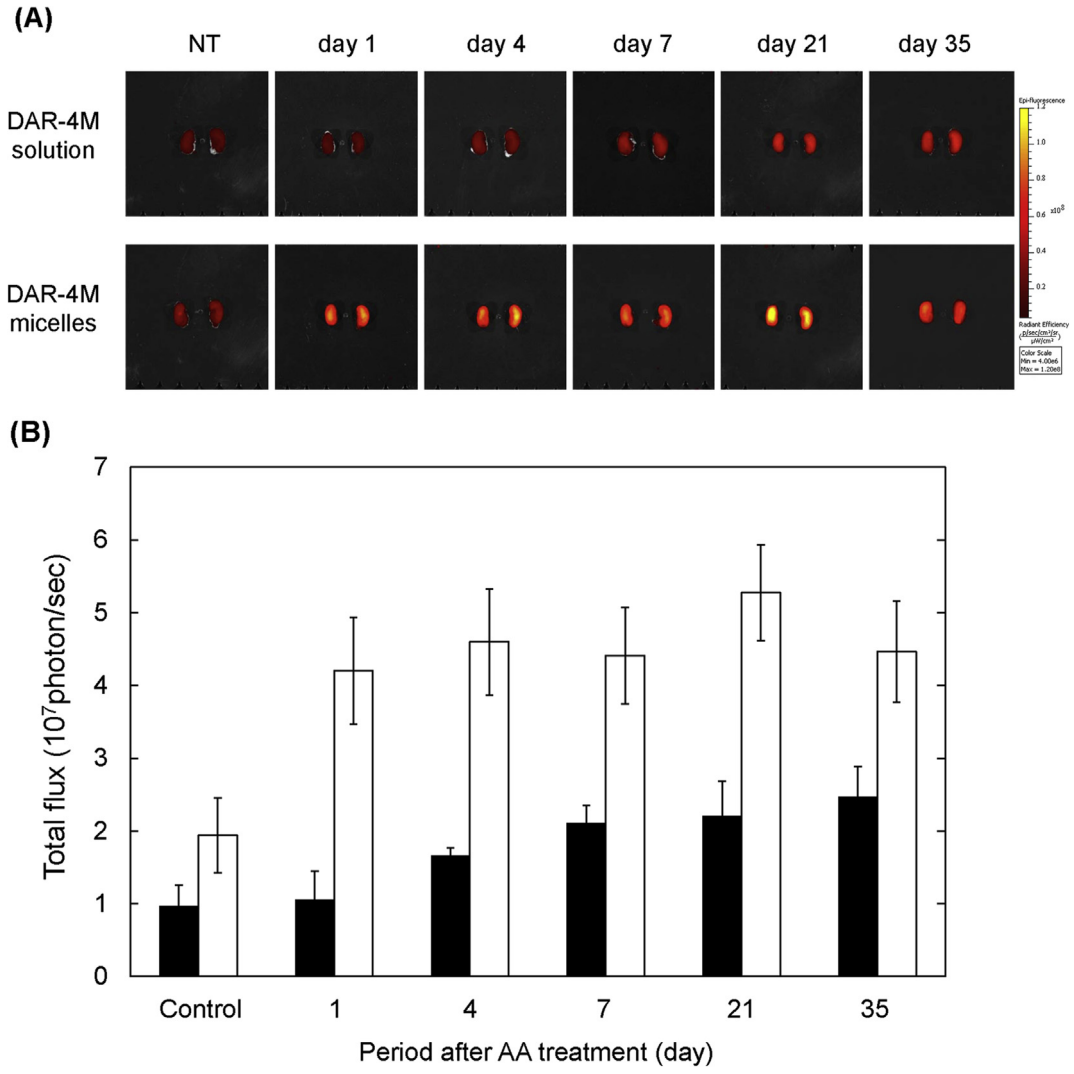

Fig. 6. IVIS analysis of isolated kidneys of mice 1 h after intravenous injection of free DAR-4M and DAR-4M micelles. Mice were treated with AA for 1, 4, 7, 21, and 35 days. The DAR-4M micelles were prepared by DSPE-10. (A) IVIS images of isolated kidney. (B) Total photon flux of isolated kidneys after intravenous injection of free DAR-4M (■) and DAR-4M micelles (□).

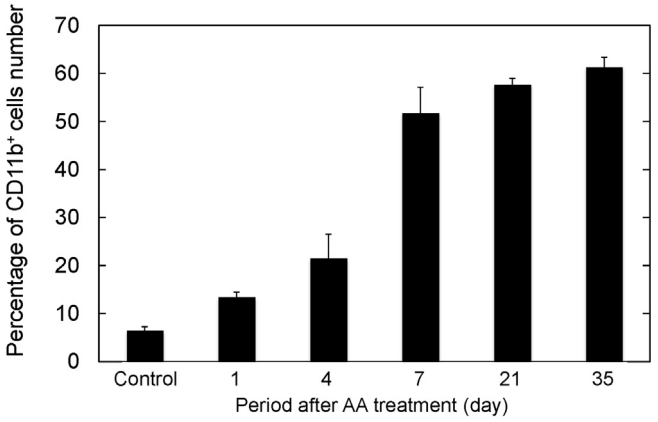

Fig. 7. Percentage of CD11b-positive cells to the total live cells in kidneys of AA-treated mice after injection of DAR-4M micelles. The DAR-4M micelles were prepared by DSPE-10. *$p < 0.05$; significance between the two groups.

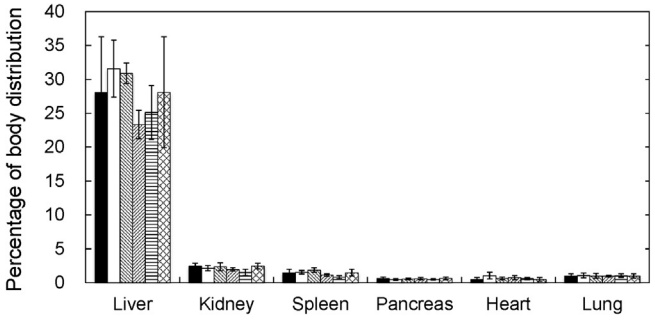

Fig. 8. Body distribution of mice 1 h after intravenous injection of ^{125}I–DAR-4M micelles. ^{125}I–DAR-4M micelles were intravenously injected to the normal (0 day after injection) (■) and AA-treated mice 1 day (□), 4 days (▧), 7 days (▨), 21 days (▤) and 35 days (▩) after injection.

membrane [13] (Fig. 3A and E). Fluorescence was also seen for LPS-stimulated cells incubated with the mixture of DSPE-g-gelatin micelles and free DAR-4M or DAR-4M micelles (Fig. 3C and D). On the other hand, no fluorescence was detected (Fig. 3B). The findings indicate that DSPE-grafted gelatin itself does not generate fluorescence. Even at the same concentration of DAR-4M added to cells, the DAR-4M micelles showed higher fluorescent intensity than free DAR-4M (Fig. 4). The DAR-4M micelles were localized inside cells (Fig. 5). We can say with certainty that the increased amount of DAR-4M in the cytosol of cells was achieved by the phagocytosis of DAR-4M micelles. The micelles phagocytosis would allow the DAR-4M to concentrate in the cells.

DAR-4M micelles imaged the inflamed kidney to a significantly great extent compared with free DAR-4M (Fig. 6). The DAR-4M incorporated into the micelles increased the amount of DAR-4M in cells. Because the phagocytosis of micelles can carry a large amount of DAR-4M into cells at one time compared with the simple permeation of free DAR-4M into cells. Moreover, the micelles formation would allow DAR-4M to stabilize in the body, prolong the half-life in the blood circulation, and increase the amount of DAR-4M in the cytosols of cells. As the result, the micelles effectively enhanced the imaging ability of DAR-4M in vivo compared with that of free DAR-4M in vivo. It is apparent from Fig. 7 that the number of CD11b-positive cells increased with time after AA treatment. This suggests that the cells were recruited into the kidney inflamed, in contrast to the normal kidney. In addition, the fluorescent intensity increased with time (Fig. 6A). On the contrary, in the normal kidney, weaker imaging was observed even for the DAR-4M micelles injection group. Taken together, it is highly possible that the DAR-4M micelles imaged CD11b-positive inflammation cells like macrophages in terms of NO production.

Little difference in the body distribution of the DAR-4M micelles was observed between the normal and inflamed kidneys (Fig. 8). On the contrary, the fluorescence intensity of kidneys was significantly different between them (Fig. 6). The findings may be explained in terms of the micelles ability to image inflammation cells. It is possible that the DAR-4M micelles localized in the inflammatory site are effectively taken up by macrophages, resulting in the superior imaging of inflammation.

It is known that although light in the visible range is routinely used for intravital microscopy, the imaging of deeper tissues (>500 μm to cm) requires the use of near infrared (NIR) light. In the body, there are hemoglobin and water which work as the major absorbers of visible and infrared light, respectively. The absorption coefficient of conventional agents is normally the lowest at the NIR region around 650–900 nm [39–42]. The excitation and emission wavelength of DAR-4M used in this study are 560 and 575 nm, respectively. This is because the kidney could not be directly imaged in live mice. Development of NO detecting agents at the excitation and emission wavelengths of NIR region is required to image the inflamed kidney in live mice.

It is recognized that there are, at least, two phenotypes of macrophages, called as M1 and M2. M1 macrophages with classically pro-inflammatory functions are superior in number in inflammatory reactions and pathogen defense [2,43,44]. On the other hands, M2 macrophages with alternatively non-inflammatory functions promote the responses of type 2 helper T cells associated with tumor progression [43], parasite infections, tissue repair [2,44], and debris removal [44–46]. If M1 and M2 can be discriminated by their imaging, it would be possible to visualize the conditions of inflammation reactions in terms of macrophages movement in vivo. Based on this idea, in this study, we tried to image M1 macrophage by using NO production. NO production is one of the markers for M1 macrophages [47]. Imaging methodology to visualize the in vivo movement of M1 macrophages and M2 macrophages will open a new field of inflammation imaging.

5. Conclusion

DAR-4M incorporated into DSPE-g-gelatin micelles could detect NO effectively in both the in vitro and in vivo systems without significant cytotoxicity. The DAR-4M of a water-insoluble drug was solubilized in water by making use of the gelatin micelles. The incorporation into the micelles allowed DAR-4M to increase the amount in cells. Moreover, the micelles formation could stabilize DAR-4M in the body, prolong the half-life in the blood circulation, and increase the amount of DAR-4M in the cytosols of cells. It is concluded that the DAR-4M micelles have an effective imaging ability in vivo compared with free DAR-4M.

Conflict of interest

There is no conflict of interest to disclose.

References

[1] Crupi A, Costa A, Tarnok A, Melzer S, Teodori L. Inflammation in tissue engineering: the Janus between engraftment and rejection. Eur J Immunol 2015;45:3222–36.
[2] Mosser DM, Edwards JP. Exploring the full spectrum of macrophage activation. Nat Rev Immunol 2008;8:958–69.
[3] Palmer RM, Ferrige AG, Moncada S. Nitric oxide release accounts for the biological activity of endothelium-derived relaxing factor. Nature 1987;327:524–6.
[4] Furchgott RF. Endothelium-derived relaxing factor: discovery, early studies, and identifcation as nitric oxide (Nobel lecture). Angew Chem Int Ed 1999;38:1870–80.
[5] Murad F. Discovery of some of the biological effects of nitric oxide and its role in cell signaling (Nobel lecture). Angew Chem Int Ed 1999;38:1857–68.
[6] Napoli C, Ignarro LJ. Nitric oxide and atherosclerosis. Nitric Oxide Biol chemistry/Official J Nitric Oxide Soc 2001;5:88–97.
[7] Coleman JW. Nitric oxide in immunity and inflammation. Int Immunopharmacol 2001;1:1397–406.
[8] Crowell JA, Steele VE, Sigman CC, Fay JR. Is inducible nitric oxide synthase a target for chemoprevention? Mol Cancer Ther 2003;2:815–23.
[9] Lim KH, Ancrile BB, Kashatus DF, Counter CM. Tumour maintenance is mediated by eNOS. Nature 2008;452. 646–U11.
[10] Wolf G. Nitric oxide and nitric oxide synthase: biology, pathology, localization. Histol Histopathol 1997;12:251–61.
[11] Griffith OW, Stuehr DJ. Nitric oxide synthases: properties and catalytic mechanism. Annu Rev Physiol 1995;57:707–36.
[12] Kobayashi Y. The regulatory role of nitric oxide in proinflammatory cytokine expression during the induction and resolution of inflammation. J Leukoc Biol 2010;88:1157–62.
[13] Kojima H, Hirotani M, Nakatsubo N, Kikuchi K, Urano Y, Higuchi T, et al. Bioimaging of nitric oxide with fluorescent indicators based on the rhodamine chromophore. Anal Chem 2001;73:1967–73.
[14] Kojima H, Nakatsubo N, Kikuchi K, Kawahara S, Kirino Y, Nagoshi H, et al. Detection and imaging of nitric oxide with novel fluorescent indicators: diaminofluoresceins. Anal Chem 1998;70:2446–53.
[15] Kojima H, Sakurai K, Kikuchi K, Kawahara S, Kirino Y, Nagoshi H, et al. Development of a fluorescent indicator for nitric oxide based on the fluorescein chromophore. Chem Pharm Bull 1998;46:373–5.
[16] Miles AM, Wink DA, Cook JC, Grisham MB. Determination of nitric oxide using fluorescence spectroscopy. Methods Enzym 1996;268:105–20.
[17] Zhang X, Zhang HS. Design, synthesis and characterization of a novel fluorescent probe for nitric oxide based on difluoroboradiaza-s-indacene fluorophore. Spectrochimica Acta Part A, Mol Biomol Spectrosc 2005;61:1045–9.
[18] Kobayashi H, Choyke PL. Target-cancer-cell-specific activatable fluorescence imaging probes: rational design and in vivo applications. Accounts Chem Res 2011;44:83–90.
[19] Gupta AK, Gupta M. Synthesis and surface engineering of iron oxide nanoparticles for biomedical applications. Biomaterials 2005;26:3995–4021.
[20] Torchilin VP. Multifunctional nanocarriers. Adv Drug Deliv Rev 2006;58:1532–55.
[21] McCarthy JR, Bhaumik J, Karver MR, Sibel Erdem S, Weissleder R. Targeted nanoagents for the detection of cancers. Mol Oncol 2010;4:511–28.
[22] Tabata Y, Ikada Y. Protein precoating of polylactide microspheres containing a lipophilic immunopotentiator for enhancement of macrophage phagocytosis and activation. Pharm Res 1989;6:296–301.
[23] Tanigo T, Takaoka R, Tabata Y. Sustained release of water-insoluble simvastatin from biodegradable hydrogel augments bone regeneration. J Control Release Official J Control Release Soc 2010;143:201–6.

[24] Katewa SD, Katyare SS. A simplified method for inorganic phosphate determination and its application for phosphate analysis in enzyme assays. Anal Biochem 2003;323:180–7.
[25] Goddard ED, Turro NJ, Kuo PL, Ananthapadmanabhan KP. Fluorescence probes for critical micelle concentration determination. Langmuir ACS J Surfaces Colloids 1985;1:352–5.
[26] Sato N, Takahashi D, Chen SM, Tsuchiya R, Mukoyama T, Yamagata S, et al. Acute nephrotoxicity of aristolochic acids in mice. J Pharm Pharmacol 2004;56:221–9.
[27] Hirsch LR, Stafford RJ, Bankson JA, Sershen SR, Rivera B, Price RE, et al. Nanoshell-mediated near-infrared thermal therapy of tumors under magnetic resonance guidance. Proc Natl Acad Sci U. S. A 2003;100:13549–54.
[28] Wilbur DS, Hadley SW, Hylarides MD, Abrams PG, Beaumier PA, Morgan AC, et al. Development of a stable radioiodinating reagent to label monoclonal antibodies for radiotherapy of cancer. J Nucl Med Official Publ Soc Nucl Med 1989;30:216–26.
[29] Maurin M, Stephan O, Vial JC, Marder SR, van der Sanden B. Deep in vivo two-photon imaging of blood vessels with a new dye encapsulated in pluronic nanomicelles. J Biomed Opt 2011;16:036001.
[30] Tong R, Coyle VJ, Tang L, Barger AM, Fan TM, Cheng J. Polylactide nanoparticles containing stably incorporated cyanine dyes for in vitro and in vivo imaging applications. Microsc Res Tech 2010;73:901–9.
[31] Wu L, Fang S, Shi S, Deng J, Liu B, Cai L. Hybrid polypeptide micelles loading indocyanine green for tumor imaging and photothermal effect study. Biomacromolecules 2013;14:3027–33.
[32] Zhang Z, Xiong X, Wan J, Xiao L, Gan L, Feng Y, et al. Cellular uptake and intracellular trafficking of PEG-b-PLA polymeric micelles. Biomaterials 2012;33:7233–40.
[33] Tabata Y, Ikada Y. Macrophage activation through phagocytosis of muramyl dipeptide encapsulated in gelatin microspheres. J Pharm Pharmacol 1987;39:698–704.
[34] Doi N, Jo JI, Tabata Y. Preparation of biodegradable gelatin nanospheres with a narrow size distribution for carrier of cellular internalization of plasmid DNA. J Biomaterials Sci Polym Ed 2012;23(8):991–1004.
[35] Matsumura Y, Maeda H. A new concept for macromolecular therapeutics in cancer chemotherapy: mechanism of tumoritropic accumulation of proteins and the antitumor agent smancs. Cancer Res 1986;46:6387–92.
[36] Maeda H, Nakamura H, Fang J. The EPR effect for macromolecular drug delivery to solid tumors: improvement of tumor uptake, lowering of systemic toxicity, and distinct tumor imaging in vivo. Adv Drug Deliv Rev 2013;65:71–9.
[37] Sato H, Fujiwara M, Bannai S. Effect of lipopolysaccharide on Transport and metabolism of arginine in mouse peritoneal-macrophages. J Leukoc Biol 1992;52:161–4.
[38] Miller L, Alley EW, Murphy WJ, Russell SW, Hunt JS. Progesterone inhibits inducible nitric oxide synthase gene expression and nitric oxide production in murine macrophages. J Leukoc Biol 1996;59:442–50.
[39] Weissleder R. A clearer vision for in vivo imaging. Nat Biotechnol 2001;19:316–7.
[40] Hilderbrand SA, Weissleder R. Near-infrared fluorescence: application to in vivo molecular imaging. Curr Opin Chem Biol 2010;14:71–9.
[41] Pysz MA, Gambhir SS, Willmann JK. Molecular imaging: current status and emerging strategies. Clin Radiol 2010;65:500–16.
[42] Frangioni JV. In vivo near-infrared fluorescence imaging. Curr Opin Chem Biol 2003;7:626–34.
[43] Mantovani A, Sozzani S, Locati M, Allavena P, Sica A. Macrophage polarization: tumor-associated macrophages as a paradigm for polarized M2 mononuclear phagocytes. Trends Immunol 2002;23:549–55.
[44] Gordon S. Alternative activation of macrophages. Nat Rev Immunol 2003;3:23–35.
[45] Brown BN, Ratner BD, Goodman SB, Amar S, Badylak SF. Macrophage polarization: an opportunity for improved outcomes in biomaterials and regenerative medicine. Biomaterials 2012;33:3792–802.
[46] Novak ML, Koh TJ. Macrophage phenotypes during tissue repair. J Leukoc Biol 2013;93:875–81.
[47] Rath M, Muller I, Kropf P, Closs EI, Munder M. Metabolism via arginase or nitric oxide synthase: two competing arginine pathways in macrophages. Front Immunol 2014;5:532.